

# Nanoscale

Accepted Manuscript



This is an *Accepted Manuscript*, which has been through the Royal Society of Chemistry peer review process and has been accepted for publication.

*Accepted Manuscripts* are published online shortly after acceptance, before technical editing, formatting and proof reading. Using this free service, authors can make their results available to the community, in citable form, before we publish the edited article. We will replace this *Accepted Manuscript* with the edited and formatted *Advance Article* as soon as it is available.

You can find more information about *Accepted Manuscripts* in the [Information for Authors](#).

Please note that technical editing may introduce minor changes to the text and/or graphics, which may alter content. The journal's standard [Terms & Conditions](#) and the [Ethical guidelines](#) still apply. In no event shall the Royal Society of Chemistry be held responsible for any errors or omissions in this *Accepted Manuscript* or any consequences arising from the use of any information it contains.

## REVIEW

## Emerging double helical nanostructures

Cite this: DOI: 10.1039/x0xx00000x Meng-Qiang Zhao, Qiang Zhang\*, Gui-Li Tian, Fei Wei\*

Received 00th January 2014,  
Accepted 00th January 2014

DOI: 10.1039/x0xx00000x

www.rsc.org/

As one of the most important and land-mark structure found in nature, a double helix consists of two congruent single helices with the same axis or a translation along the axis. Such double helical structure renders the deoxyribonucleic acid (DNA) as the crucial biomolecules in evolution and metabolism. The DNA-like double helical nanostructures are probably the most fantastic yet ubiquitous geometry at nanoscale, which are expected to exhibit exceptional and even rather different properties due to the unique organization of the two single helices and their synergistic effect. The organization of nanomaterials into double helical structures is an emerging hot topic for nanomaterials science due to their promising exceptional unique properties and applications. This review focuses on the state-of-the-art research progress for the fabrication of double-helical nanostructures based on 'bottom-up' and 'top-down' strategies. The relevant nanoscale, mesoscale, and macroscopic scale fabrication methods, as well as the properties of the double helical nanostructures are included. Critical perspectives are devoted to the synthesis principles and potential applications in this emerging research area. A multidisciplinary approach from the scope of nanoscience, physics, chemistry, materials, engineering, and other application areas is still required to the well-controlled and large-scale synthesis, mechanism, property, and application exploration of double helical nanostructures.

## 1. Introduction

Helix is probably the most fantastic yet ubiquitous geometry in nature, science, art, and architectures. A helix is a type of smooth space curve, which exhibits the property that the tangent line at any point makes a constant angle with a fixed line called the axis. Therefore, the helix is a kind of structure form that can fully utilize the space while exhibits excellent structural stability and artistic beauty. Scientists have been fascinated for centuries by the ubiquitous helicity found in nature. The most important and land-mark helix structure found in nature is the deoxyribonucleic acid (DNA), which exhibits the helical arrangement of alternating sugar residues and phosphate stabilized by hydrogen bonds between the bases attached two anti-parallel polynucleotide strands. Such unique double helical structure is of paramount importance to explain why DNA plays a crucial role in evolution and metabolism. Some other biological molecules such as many proteins also adopt the helical substructures, known as  $\alpha$ -helices.

The fascinating morphology of the helix has stimulated many synthetic efforts to mimic its unique structure.<sup>1</sup> With the rapid development of nanoscience and nanotechnology, organization of micro/nanomaterials into helical configuration has become an important topic and hot issue due to its obvious impacts on the properties and the consequence promising applications of the

materials.<sup>2-5</sup> In general, bring helical configuration into micro/nanomaterials could not only provide the integration of the properties of the materials originated from their composition and unique organization, but also give rise to new opportunities to unravel natural construction rules.<sup>3-7</sup> However, the fabrication of helical micro/nanostructures is a great challenge in materials science due to the fact that the materials in micro- especially in nanoscale are always too small to be individually fabricated by the top-down lithography methods and too big to be synthesized by the well-established molecular synthesis. Recent advances in the development of materials chemistry allow better control over the size and shape of the micro/nanomaterials. Therefore, several synthetic strategies have been explored to fabricate helical micro/nanostructures upon the self-assembly of basic building blocks for both organic and inorganic materials, which often occurs without any external energy input and is driven by the energy minimization.<sup>3-5, 7-10</sup> However, in most cases, only single helical structures were successfully fabricated.

Compared to materials with single helical structure, the double helical structures could be expected to be with much better unique properties and promising applications.<sup>2, 5, 11-15</sup> The double helix consisting of two congruent single helices with the same axis or a translation along the axis, is the basic structure of DNA (Figure 1a). Therefore, the double helical structure is considered as a much basic

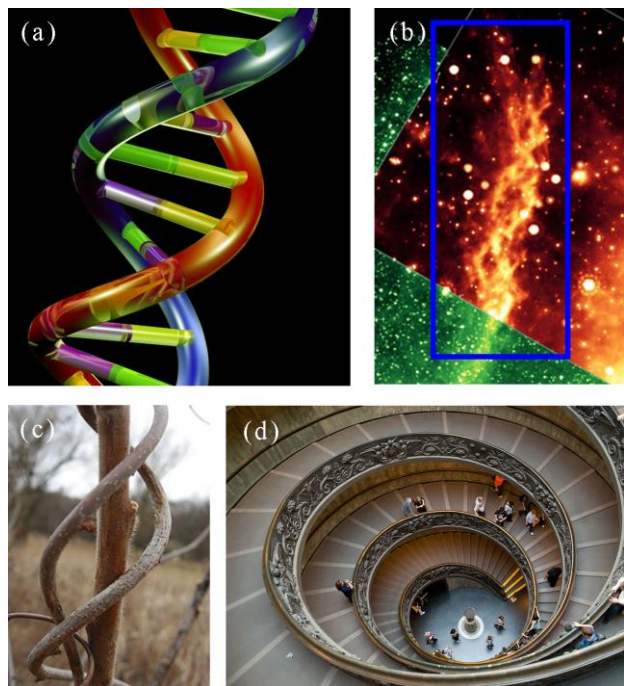


**Figure 1** (a) Model of DNA double helix; (b) Double helical galaxies; (c) Double helical stems of plant; (d) The 'double helix' staircase of the Vatican Museum.

structure for life. Nature has the unique power to create such delicate architectures spanning from nanoscale DNA molecule to macroscopic vine plant, and even to the universal galaxies (**Figure 1a-c**). The double helical staircase of the Vatican Museum is a typical instance of a perfect combination of architecture and art (**Figure 1d**). The double helical structures could exhibit exceptional and even rather different properties due to the unique organization of the two single helices and their synergistic effect. The double-helical organization of micro/nanoscale materials can not only inherit and even strengthen their intrinsic properties, but also bring extraordinary unexpected properties.<sup>2</sup> For instance, the Cao group demonstrated that the double-helical organization of CNT yarns would induce rather unique and improved mechanical properties than straight and single-helical CNT yarns.<sup>15</sup> It was also found that the helical arrangement conductive materials could give rise to exceptional electrical properties.<sup>16, 17</sup> Furthermore, unique optical and electric-magnetic properties of double helices and their corresponding applications can also be expected.<sup>2, 18, 19</sup> Therefore, the exploration of building the unique double helical architectures with either organic or inorganic building blocks has drawn intense interests. The double helical assembly can be easily fabricated from organic molecules due to their complex shapes and different kinds of inter- and intra-molecular interactions similar to that of DNA.<sup>4, 20</sup> On the contrast, the construction of inorganic nanoarchitectures always involves the direct assembly of atoms and/or ions. The symmetric shape of atoms or ions and the lack of various interactions make it much more difficult for inorganic materials to be self-assembled into helical structures. It is even a much greater challenge for materials science and chemistry to fabricate inorganic double helical structures due to it further requires the formation of two congruent inorganic

helices simultaneously that are combined together with the same axis or a translation along the axis.

In this review article, the state-of-the-art research progress and achievements on the fabrication of double helical structures is highlighted. Both the "bottom-up" and "top-down" strategies, including the nanoscale, mesoscale, and macroscopic scale methods, as well as their involved formation mechanism are discussed in detail in the next section. Then the current and promising property investigations of the as-fabricated double helices are briefly introduced. Based on our understanding of the current state in this emerging field, we try to point out the existing problems and show insight into future investigations.

## 2. Fabrication strategies

Two strategies, including both "bottom-up" and "top-down" strategies, have been developed for the fabrication of double helical micro/nanostructures. For the "bottom-up" strategy, the most straightforward method is the self-assembly of molecules into the double helical configuration through various kinds of inter/intra-molecular interactions. The assembly of nanoparticles (NPs) under the direction of double helical organic templates or under the controlled growth mode are also effective for the formation of double helical structures. Besides, the physical confinement in nano/micropores can also lead the organization of atoms or organic molecules into a double helical configuration. Until recently, it is demonstrated that double helical inorganic structures, mainly referring to carbon micro/nanostructures, can be directly fabricated through the catalytic deposition methods beyond solutions. On the other hand, the development of nanotechnology and nanomanipulation allows better control over the morphology of micro/nanomaterials. Several strategies, such as the nanoscale chemical modification, microscale transformation under capillary force, and macroscopic process, have been proposed to fabrication double helical structures through the "top-down" strategy.

### 2.1 Bottom-up strategy

#### 2.1.1 Molecular self-assembly

The self-assembling of molecules into a double helical configuration is considered as the most straightforward method for the fabrication of double helical structures. In addition to the building blocks for those biological motives with double helical morphology (e.g. DNA and some proteins), most of the small organic molecules that can self-assemble into the double-helical structures are amphiphilic.<sup>21, 22</sup> As the most common groups of amphiphilic molecules, lipids and their analogues are one of the mostly used building blocks for the self-assembly of double helical nanostructures. For instance, Yanagawa *et al.* synthesized a phospholipid-nucleoside conjugate containing two long alkyl chains and a nucleotidyl residue, dimyristoyl-5'-phosphatidyl-deoxycytidine, and found the self-assembled double-helical structure in aqueous solution.<sup>23</sup> Oda *et al.* reported that cationic Gemini surfactants affording chiral tartrate counter ions for self-assembly of double helices both in chlorinated

and aromatic organic solvents, and in water.<sup>24</sup> The handedness and helical pitch of the double helical ribbons were tuned upon varying the ratio between  $L$  and  $D$  tartrate. By designing a functional amphiphilic molecule bearing a sugar moiety, azobenzene group and butyl chain ( $C_4AG$ ), Lin *et al.* reported the successful fabrication of one-dimensional intertwined double helices that were composed of nanofibers in aqueous solution.<sup>25, 26</sup> The self-assembled double helices were demonstrated to be stable with respect to dilution, heat, urea and organic solvent. It was suspected that the helicity of the self-assembled fibers were originated from the staggered stacking of the amphiphilic molecules, and the driven force for the self-organization of the double helical configuration was ascribed to the virtue of multiple non-covalent interactions, such as hydrophobic interaction, aromatic stacking, and hydrogen bond.

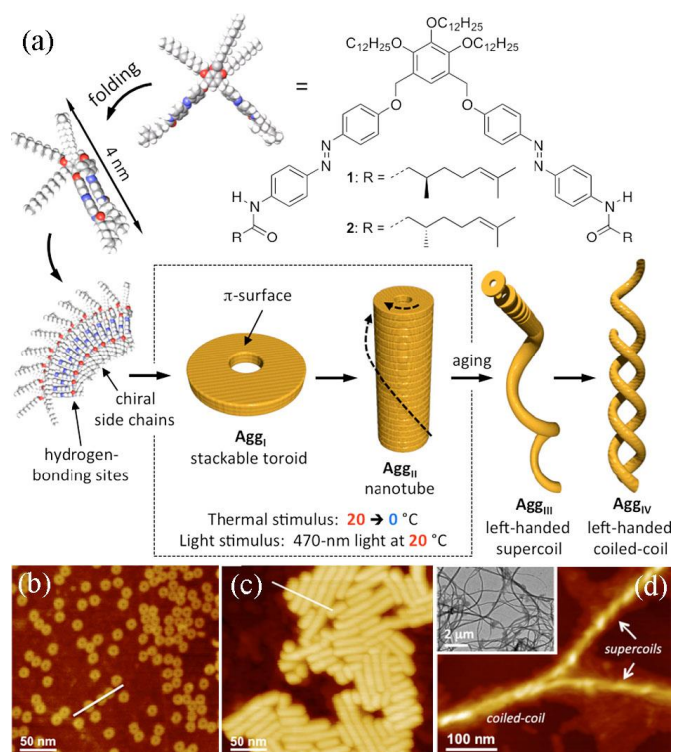


**Figure 2** (a) Schematic representation of the hierarchical self-assembly of the chiral azobenzene dimer; (b) Atomic force microscopy height images of (b) toroidal aggregates  $Agg_I$ , (c) tubular aggregates  $Agg_{II}$  and (d) helical aggregates  $Agg_{III}$  and  $Agg_{IV}$ . Inserted image in (d) is the TEM image of helical aggregates  $Agg_{III}$  and  $Agg_{IV}$ .<sup>27</sup> Reprinted with permission from Ref. 27. Copyright 2012 from American Chemical Society.

In the case of small molecules that are not amphiphilic, combining two or more kinds of such organic molecules together to form amphiphilic block copolymers is a promising way for achieving the overall double helical morphology. Pochan *et al.* reported that the self-assembly of poly(acrylic acid)-*b*-poly(methyl acrylate)-*b*-polystyrene (PAA-PMA-PS) in the presence of multiamines led to both single and double helical structures.<sup>28</sup> It was proposed that the charge neutralization by multiamines that caused the axial concentration of the PAA domain acted as the reason for

the buckling and twisting of the PS domain into helices. Emrick *et al.* found the formation of a mixture of single, double, and quadruple helices through the co-assembly of poly(3-hexylthiophene)-*b*-poly(3-triethylene glycol thiophene) (P3HT-P3(TEG)T) upon the presence of  $K^+$  ions.<sup>29</sup> The authors proposed that it could be the  $K^+$  ions that induced the staggered stacking of P3HT, which resulted in the twisting of the overall superstructure into helical morphologies. The Liu group designed a poly(*n*-butyl methacrylate)-*b*-poly-(2-cinnamoyloxyethyl methacrylate)-*b*-poly(*tert*-butyl acrylate) (PBMA-PCEMA-PtBA) copolymer, which can self-assemble into double and triple helices over a long period.<sup>20, 30</sup> The formation of the helices was proposed to be driven by the tendency to reduce the PBMA/solvent interface. Besides, Jinnai *et al.* reported the visualization of a three-dimensional double helical morphology for a polystyrene-*b*-polybutadiene-*b*-poly(methyl methacrylate) (PS-PB-PMMA) triblock terpolymer, which was composed of PB helical domains around hexagonal-packed PS cylinder cores in a PMMA matrix.<sup>31, 32</sup> The orientation of such triblock polymer double helices was achieved through following solvent annealing and drying at a controlled solvent evaporation rate.<sup>31</sup>

It should be noted that the self-assembly of organic molecules into double helical structures is always constructed along with more complicated self-organization schemes than expected. On one hand, a long aging process is always required. Take the assembly of PBMA-PCEMA-PtBA triblock copolymer for instance, it was found that only cylindrical aggregates together with spherical aggregates could be observed after 1 day of sample aging. After 8 days, longer cylinders could be obtained. The cylinders started to transform into the single helical morphology after 16 days. It was until after 24 days that double helices were available, which became the major configuration after 3 months.<sup>20</sup> On the other hand, the self-assembly process always undergoes hierarchy levels with different kinds of intermediate morphologies. As mentioned above, spherical aggregates, cylinders, and single helical morphologies existed during the aging of the double helices.<sup>20</sup> Besides, Yagai *et al.* reported a precise control over the hierarchy levels in the outstanding process of double helices using a chiral azobenzene dimer (**Figure 2a**).<sup>27</sup> It was found that the compound formed uniform toroidal nanostructures first (**Figure 2b**), which were then hierarchically organized into chiral nanotubes under the control by temperature, concentration, or light (**Figure 2c**). The nanotubes further assembled into supercoiled fibers, and finally intertwined to form double helical structures with one-handed helical sense (**Figure 2d**). Furthermore, the external conditions during the molecular self-assembly also plays an important role in the successful formation of double helical structures. For instance, Lin *et al.* found that the double helical configuration built up by  $C_4AG$  could be shaped into spherical micelles, vesicles or unfolded nanofibers by external stimuli, such as pH, light, and surfactant addition.<sup>25, 26</sup> Such morphology transformation could be attributed to the changing of molecular hydrophilicity and electrostatic repulsion upon external stimuli, which were considered to be of paramount importance for the organization of double helical structures.

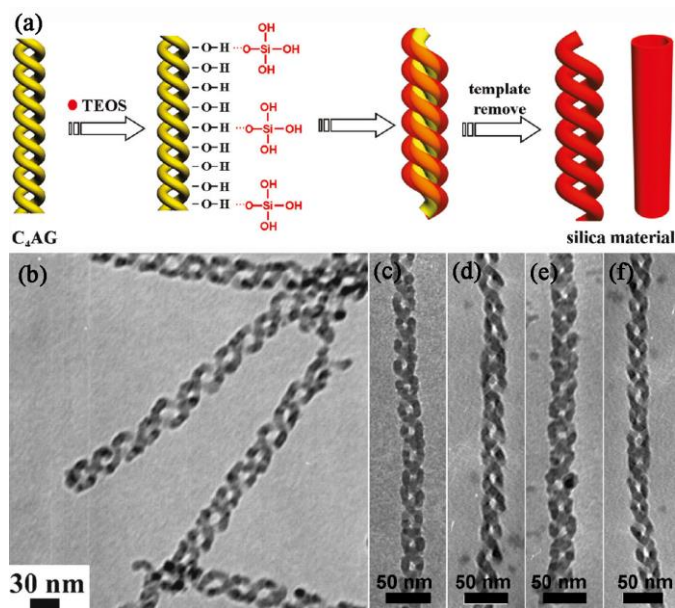


**Figure 3** (a) Possible scheme of sol-gel reaction into double helical  $\text{SiO}_2$  nanostructures with  $\text{C}_4\text{AG}$  amphiphile and surfactant as templates; TEM image of the as-prepared double helical  $\text{SiO}_2$  template from  $\text{C}_4\text{AG}$  solution with different molar ratios of  $\text{C}_4\text{AG}/\text{TEOS}/\text{NH}_3$ : (b, c) 1:9:4; (d) 1:9:5; (e) 1:9:6; (f) 1:9:7. The concentration of  $\text{C}_4\text{AG}$  solution is fixed at 5 mM.<sup>25</sup> Reprinted with permission from Ref. 25. Copyright 2008 from American Chemical Society.

The fabrication of inorganic materials with double helical configuration can also be achieved through the molecular self-assembly method. Regarding to this, perhaps the most well-known and well-investigated system is the preparation of helical mesoporous silica, which involves the co-assembly of amphiphilic surfactants and silica precursors (e.g. tetraethyl orthosilicate (TEOS)) or the template assembly of silica precursors through electrostatic interactions.<sup>33-36</sup> Due to the outside hydrophilic groups can have strong interactions with inorganic materials in terms of electrostatic interaction, helical micelles and micelle-like materials are considered to be an ideal template for the fabrication of helical and even double helical materials.<sup>37</sup> In most cases, such helical mesoporous silica exhibits the morphology of helical ribbons with helical mesoporous channels inside and single-helical tapes.<sup>33</sup> However, with precise control of the precursors and the reaction parameters, mesoporous silica with double helical structures can also be available. Wu *et al.* achieved the preparation of racemic double helical mesoporous silica using achiral surfactant sodium dodecyl sulfate (SDS) as the template, N-trimethoxysilylpropyl-N,N,N-trimethylammonium chloride as the co-structure-directing agent, and TEOS as the silica source.<sup>38</sup> On the other hand, Jung *et al.* found that sugar-based gelator *p*-dodecanoyl-aminophenyl- $\beta$ -D-glucopyranoside can self-assemble into double-helical fibers with diameters of 3-25 nm and lengths of several micrometers in the presence of *p*-aminophenyl glucopyranoside.<sup>39</sup> The amine moiety of *p*-aminophenyl glucopyranoside serves as a binding site for TEOS, and induces the transcription of the double helical structure of the organic assemblies into double-helical silica nanotubes. Similarly, many other organic

double helical templates have been transcribed to fabricate silica double helices.<sup>25, 40-42</sup> It should be noted that silica double helices with different chirality can be obtained when using exclusive left- or right-handed organic templates. Lin *et al.* found that the self-assembled double helices in  $\text{C}_4\text{AG}$  solution are exclusive left-handed. When exploited as soft template, chiral left-handed silica double helices were readily prepared (**Figure 3**).<sup>25</sup> It was demonstrated that the transcription conditions, including the concentration of the catalyst, temperature, and the ratio of alcohols to water, were important for the successful fabrication of silica double helices, as they were able to induce the morphology transformation of the organic templates.<sup>25, 40</sup>

The direct assembly of molecules can also give rise to double helical morphology even without the assistance of templates. Solution based reactions, such as hydrothermal synthesis, have been widely used in the preparation of inorganic nanostructures with well-controlled morphologies following the as-called “bottom-up” strategy. Upon the hydrothermal treatment of structurally simple precursors, including  $\text{KVO}_3$ , V,  $\text{H}_3\text{PO}_4$ ,  $\text{CH}_3\text{PO}(\text{OH})_2$ ,  $(\text{CH}_3)_2\text{NH}$ , and  $\text{H}_2\text{O}$ , in a well-designed mole ratio, Soghomonian *et al.* prepared very complicated inorganic solids,  $[(\text{CH}_3)_2\text{NH}_2]\text{K}_4[\text{V}_{10}\text{O}_{10}(\text{H}_2\text{O})_2(\text{OH})_4(\text{PO}_4)_7]\cdot 4\text{H}_2\text{O}$ , which were a kind of vanadium phosphate containing double helices formed from interpenetrating spirals of vanadium oxo pentamers bonded together by  $\text{P}^{5+}$ .<sup>43</sup> The optimized synthetic conditions for the formation of inorganic double helix were determined empirically after the observation of the products in other reactions with the same starting materials but with different molar ratios. The formation mechanism of the double helical vanadium phosphate was not well-addressed, however, the methylphosphonic acid was crucial to the high yield synthesis of the double helical structure even though it was not incorporated into the products.

### 2.1.2 Nanoparticle assembly

The assembly of NPs or nanocrystals, either templated by organic templates or through a self-assembly process, has been explored as an efficient method for the fabrication of inorganic double helical nanostructures. For the template assembly of NPs, it always involves the deposition or reaction of inorganic cations on the surface of organic templates to form NPs or nanostructures with a double helical configuration. Nevertheless, the self-assembly of NPs or nanocrystals into double helical structures always undergoes a controlled anisotropic growth process.

As one of the most well-known double helical materials, DNA can serve as excellent platform for the double-helical assembly of metal NPs.<sup>44-47</sup> Due to their high affinity to NPs, DNA-mediated assembly of NPs is an attractive way to organize both metallic and semiconducting NPs into various architectures through the programmable base-pairing interactions and the ability to construct branched DNA nanostructures of various geometries. By attaching Au NPs with single-stranded DNA, Sharma *et al.* fabricated nanotubes of various three-dimensional (3D) architectures ranging from stacking rings to single helices, double helices, and nested helices.<sup>48</sup> Although the stacked rings were major conformations in

most cases and the incorporation of stem loops on the opposite surface side as a counterforce to resist tube formation rendered the single helix more favorable, Au NPs with double helical morphology were observed in all of as-fabricated nanostructures. In recent years, polymerase chain reaction (PCR) with DNA as the bridges has been explored as an essential tool for the well-programmed assembly of both organic and inorganic NPs.<sup>49</sup> Numerous kinds of structures were fabricated based on the PCR, including branched superstructures, Y-shaped nanostructures, and chiral assembly.<sup>49-52</sup> This reveals that the PCR could be explored as a potential and effective method for the double-helical assembly of NPs.

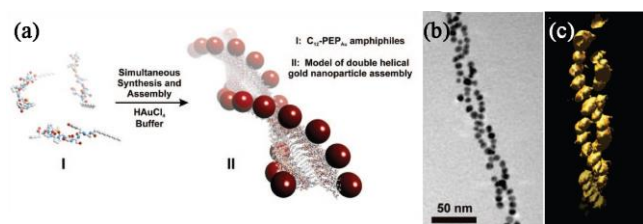


**Figure 4** (a) Schematic depiction of the formation of gold NP double helices; (b) Transmission electron microscopy (TEM) image of Au NP double helix on a helical polypeptide superstructure; (c) Electron tomography image of a similar double helix showing a 3-D surface rendering of the tomographic volume.<sup>53</sup> Reprinted with permission from Ref. 53. Copyright 2008 from American Chemical Society.

In addition to DNA, peptides are also usually adopted as the templates for the organization of metal NPs into double helical morphology. With the research developments on the investigation and manipulation of peptide self-assembly and the *in vitro* evolution of specific peptides for mineralizing and recognizing specific inorganic materials, Chen *et al.* reported a one-pot direct approach that coupled peptide self-assembly and peptide-based biomineralization into one simultaneous process and prepared an unprecedented left-handed Au NP double-helical structures using this method (**Figure 4**).<sup>53</sup> A specific peptide with the hydrophobic tail squeezed at the center and the hydrophilic polypeptide on the surface was designed and self-assembled into left-handed helical ribbons. Au NPs were deposited on the surface of the helical ribbons after the reduction of HAuCl<sub>4</sub> and self-assembled into left-handed double helix configuration. The structural parameters of the double helical Au NPs were controlled in terms of the size of the Au NPs, the inter-helical separation, and the formation of the continuous one-dimensional (1D) metal superstructure. Further study revealed that chiral Au NP double helices with selective handedness were prepared through using the peptide template with different chiralities.<sup>54</sup>

It is interesting that micelles with a tubular morphology were used as the template for the assembly of NPs to fabricate double helical nanostructures.<sup>55-57</sup> Lipid nanotubes are a typical kind of hollow cylindrical micelles, which are composed of helically coiled bilayer ribbons. Price *et al.* fabricated nanoscale metal coils using an electroless metallization approach based on the general concept to exploit helical seam features of self-assembled diacetylenic

phospholipid microtubules as templates.<sup>58</sup> Such metallization templates were created through selective and sequential absorption of the oppositely charged polyelectrolytes, sodium poly(styrenesulfonate), and poly(ethyleneimine) (PEI) onto nanoscale double helical seams naturally occurring on the microtube surface. The selective template formation of double helical Cu nanostructures was initiated and catalyzed by negatively charged Pd(II) NPs that were bounded to the terminal cationic PEI layer of the multilayer film. Although the authors just demonstrated the use of Cu to form these double helical nanostructures, the possibility existed to utilize other metals such as Co, Ni, Fe, Ag, Au, or their alloys to vary the electrical, magnetic, and chemical properties of the resulting structures.

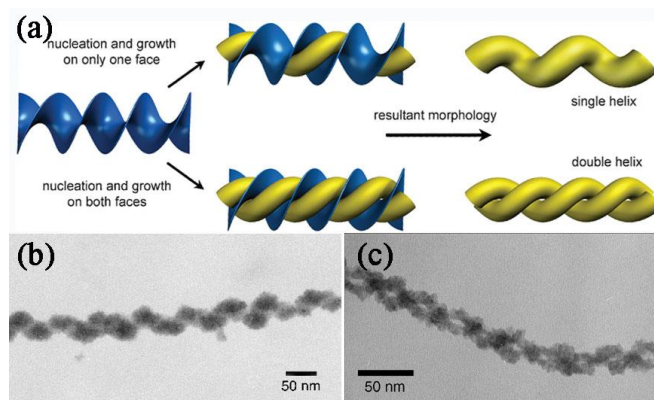


**Figure 5** (a) Schematic representation of templating pathways. Nucleation and growth on one side of the twisted ribbons (blue) leads to single helices of CdS (yellow), while nucleation and growth on both sides of the ribbon leads to double helices; TEM images of a CdS (b) single helix and (c) double helix.<sup>60</sup> Reprinted with permission from Ref. 60. Copyright 2005 from Wiley-VCH.

Compounds with a similar structure to lipids, which self-assemble into helical organic fibers, were also found to be effective for the template assembly of double helical inorganic nanostructures.<sup>39, 61-64</sup> The Stupp group reported on molecules with a triblock architecture termed “dendron rodcoils” self-assembled into ribbons with a helical structure in ethyl methacrylate.<sup>59, 60</sup> Upon addition of a cadmium nitrate solution in tetrahydrofuran (THF) as a precursor, the hydrophilic region of such ribbons (the hydroxyl-containing dendron portion) showed preferred affinity of Cd<sup>2+</sup> ions (solvated in THF), which produced a local supersaturation of ions around the ribbons and induced the nucleation and growth of CdS crystals localized at the surface of the ribbons after exposure to hydrogen sulfide gas (**Figure 5a**). Although single-helical CdS structures were the major products in most cases (**Figure 5b**), further study revealed that when mineralizing ribbons from gels that had been aged for several months, large numbers of double helical CdS structures were observed (**Figure 5c**). The structural diversity between different ribbons led to the CdS with various nanostructures.<sup>60</sup> In ribbons with a perfect twisted structure, for instance, both faces of the ribbon are equivalent, and equally able to nucleate and grow CdS, leading to the formation of double helical

CdS nanostructures. However, twisted ribbons with a slightly coiled axis have one face more exposed to the solvent, and thus are more susceptible to CdS nucleation and subsequent growth, leading to the formation of single helical CdS structures.

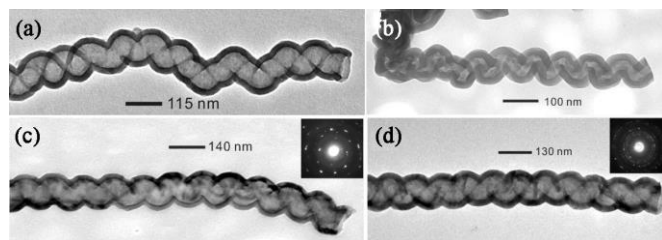


**Figure 6** TEM images of the as-fabricated helical by (a)  $\text{Al}_2\text{O}_3$ , (b)  $\text{SiO}_2$ , (c)  $\text{TiO}_2$ , and (d)  $\text{ZnAl}_2\text{O}_4$  by ALD the oxides on the surface of helical CNFs.<sup>65</sup> Reprinted with permission from Ref. 65. Copyright 2010 from Wiley-VCH.

The assembly of inorganic NPs or nanocrystals on organic double-helical fibers to form inorganic double-helical nanostructures was achieved mainly due to the strong electrostatic interactions between the inorganic materials and the surface of the organic fibers. When it applies to inorganic templates, things are quite different, which mainly involves adsorption interaction. Double-helical inorganic structures that exhibit strong affinity to other organic materials and are facile to be removed. They can also be employed as templates for the NP assembly to fabricate other kinds of inorganic double-helical structures. Due to their much better thermal and chemical stability, harsher conditions were applied on the inorganic templates compared with those using organic templates.

Carbon nanofibers (CNFs) with double helical structure are the mostly studied and adopted inorganic templates for the NP assembly to fabricate inorganic double helical nanostructures due to their strong adsorption ability of salts and the easiness of removal through oxidation process. The Ueda group successfully demonstrated that oxide nanotubes ( $\text{ZrO}_2$ ,  $\text{Al}_2\text{O}_3$ ,  $\text{SiO}_2$ ) can be available using helical CNFs as the templates through infiltrating the precursor solution into the free space of the fibrous structure.<sup>66</sup> A thin oxide and hydroxide film coating on the surface of the helical CNF templates can be obtained after hydrolyzing the absorbed precursors by the water vapor in air. The CNF templates were then removed by calcination in air at high temperatures, leaving the helical oxide nanotubes as the products. The shape of the as-fabricated oxide nanotubes was well controlled upon replicating the surface morphology of the CNF templates, and the oxide nanotubes with double helical morphology can be fabricated. Using the atomic layer deposition technique, Qin *et al.* also achieved the fabrication of various double-helical oxide nanotubes ( $\text{Al}_2\text{O}_3$ ,  $\text{SiO}_2$ ,  $\text{TiO}_2$ ,  $\text{HfO}_2$ , and  $\text{ZnAl}_2\text{O}_4$ ) using double helical CNFs as the templates (**Figure 6**).<sup>65</sup> The double helical morphology of the templates was well transcribed in the as-fabricated double helical nanotubes, which were with well-controlled thickness and excellent conformity.

If organic compounds that afforded strong interaction with the NPs or nanocrystals to alter their growth kinetic were added into the

reaction system, staggered stacking or anisotropic growth mode of the inorganic materials was achieved to form a helical and even double helical morphology.<sup>6, 67-70</sup> Zhu *et al.* firstly reported that the preparation of distinctive  $\text{BaCO}_3$  nanofibers with double-stranded helical structures was achieved through the biomimetic mineralization process on an organosilane-coated substrate *via* crystallization and controlled by a phosphonated block co-polymer.<sup>71</sup> The double-stranded helices were as long as several millimeters and were visible under an optical microscope. They were composed of pairs of single helices overlapped each other closely as a single helical coiling, most of which were 20-50  $\mu\text{m}$  in length and 0.2-2  $\mu\text{m}$  in diameter. It was demonstrated that there were two droplet-like growth points at the tip of the double-stranded helical nanofibers. During the growth of the  $\text{BaCO}_3$  fibers, the negative phosphonated block co-polymer preferentially deposits on to the positive (110) face of the primary building blocks. As a result, the formation of the double helical superstructures relied on two processes: (a) the exclusive polymer absorption onto favorable (110) faces that led to a staggered arrangement of aggregating NPs; (b) in the perpendicular direction, a particle approaching an aggregate also rendered favorable and unfavorable adsorption sites, and the change from a (020)-(020) to a (011)-(011) aggregate led to a helical coiling in the particle aggregation. An overlay of these two processes led to the formation of double helices.

### 2.1.3 Physical confinement

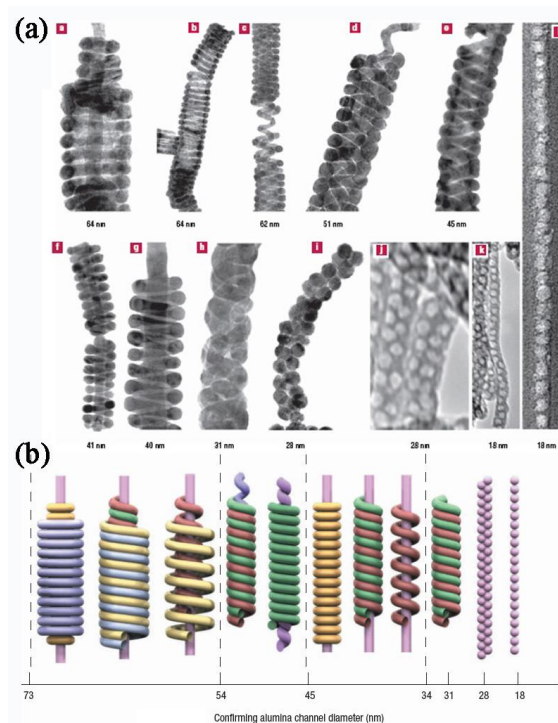


**Figure 7** (a) Representative TEM images of mesostructures formed inside PAA nanochannels with differing confinement dimensions; (b) Summary of the experimentally observed confined mesostructural evolution with varying alumina nanochannel diameters.<sup>72</sup> Reprinted with permission from Ref. 72. Copyright 2004 from Nature Publishing Group.

It is well known that when forcing a wire into a cylinder, it always comes to the situation that the external force drives the axial contraction of the wire, causing it to pack and form a helix.<sup>5</sup> Similarly, in a physically confined environment, interfacial interactions, symmetry breaking, structural frustration, and confinement-induced entropy loss can play dominant roles in determining molecular or atoms organization, which is possible to lead to a micro/nanoscale double helical configuration. Porous anodic alumina (PAA) is a template which provides ideal physical confining environment with well-controlled size. Wu *et al.* presented a systematic study of the confined assembly of silica-surfactant composite mesostructures within cylindrical nanochannels of PAA with varying diameters.<sup>72</sup> A variety of helical mesoporous silica structures were obtained after the removal of the surfactant and PAA substrate, and their morphologies were dominantly depended on the diameter of the PAA channels (**Figure 7**). When the diameter of the channels was above 34 nm, coaxial multi-layered straight cylinders, helices, and parallel stacked rings were available, among which mesoporous silica with a double helical configuration can be observed at the outer layer. When the diameter of the PAA channels decreased to *ca.* 31 nm, unique single-layered double helical silica structures were obtained. Further decrease of the diameter of the PAA channels led to the formation of double- or single-line silica spheres.

CNTs are another kind of material that can provide ideal physically confining environment for the helical configuration of atoms or chemical compounds. The field in the area of research on CNT-based hybrid nanomaterials after atom, molecule or chemical compound filling of CNTs has attracted extensive attentions.<sup>73-75</sup> Using molecular dynamics simulations, Lv *et al.* predicted that a DNA-like double helix of two poly(acetylene) chains was available inside single-walled CNTs.<sup>73</sup> The physical confinement of the inner cavity of single-walled CNTs allowed the self-assembled polymer chains to adopt a helical configuration in a single-walled CNT through the combined action of the van der Waals potential well and the  $\pi$ - $\pi$  stacking interaction between the polymer and the inner surface of single-walled CNTs. This work shed a light on the fabrication of helical structures using the inner cavity of CNTs. Later on, the Khlobystov group reported the synthesis of helically twisting graphene nanoribbons from small sulfur-containing molecules by heat treatment or electron beam in CNTs with internal diameters between 1 and 2 nm, indicating inorganic atoms can also adopt a helical configuration under the physical confinement in CNTs.<sup>75</sup> Recently, Fujimori *et al.* successfully achieved the production of covalently bonded selenium double helices with in the narrow cavity inside DWCNTs with a typical inner diameter of  $\sim$ 1 nm by exposing open-ended DWCNTs to sublimed elemental Se (**Figure 8**).<sup>74</sup> Although the formation mechanism was not well-addressed, it was demonstrated that the diameter of the inner cavity of the CNTs played dominant roles in the successful double helical organization of the Se atoms.

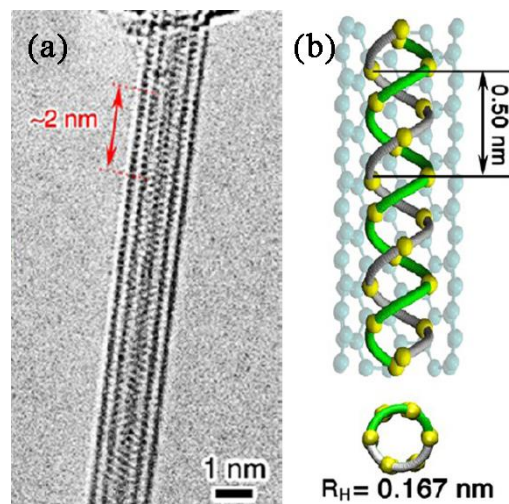


**Figure 8** (a) High-resolution TEM image revealing the Se double-helix structure with a pitch length of  $\sim$ 2 nm inside a DWCNT; (b) The optimized structure of a free-standing double-helix structure of selenium inside the (5,5) CNT.<sup>74</sup> Reprinted with permission from Ref. 74. Copyright 2013 from American Chemical Society.

#### 2.1.4 Catalytic deposition

The catalytic chemical vapor deposition (CVD) growth of nanostructures is a huge field for material synthesis beyond solutions.<sup>76-78</sup> A wide variety of structural features involving many types of materials can be fabricated by tuning the reaction parameters, such as temperature, pressure, composition of gases and their flow rate, during the CVD. In most cases, catalyst particles are used to catalyze the direct growth of inorganic materials, the shape and anisotropic reactivity of which play an important role in determining the final morphology of the as-fabricated nanostructures. Therefore, it is not surprised to obtain helical nanostructures by the catalytic deposition methods. In particular, when two wires or stands grow from different sides of individual catalyst nanoparticle, double helical structures can be expected.

##### 2.1.4.1 Carbon fiber double helices

As a typical one-dimensional carbon material, carbon fibers with helical configurations are probably among the first inorganic double-helical materials that have been extensively investigated. Catalytic CVD methods are one of the mostly used strategies for the growth of carbon fibers. In terms of tuning the composition and shape of the catalyst particles and the reaction parameters during CVD, the structural geometry of the as-grown carbon fibers can be well controlled. Generally, the anisotropic growth of carbon fibers from a catalyst particle would induce the formation of double helical configuration.<sup>7, 79</sup>

As early as 1970s, Baker *et al.* reported the catalytic growth of double helical carbon fibers using Sn/Fe alloy as the catalysts by decomposition of acetylene.<sup>80</sup> It was found that on each catalyst particle, it always came to the situation that two carbon fibers would grow with identical rates by opposite chirality of the helices, which resulted in the formation of double helical structure. The most

influential works about the double helical carbon fibers, including their preparation conditions, morphology, and extension characteristics, were carried out by the Motojima groups.<sup>16, 81-85</sup> In most cases, the preparation of the double helical carbon fibers was carried out upon the decomposition of acetylene on Ni catalyst particles. Carbon fibers or carbon nanofibers (CNFs) grew simultaneously from the catalyst particles and then coiled into double helical structures, in which the shape of Ni particles played a paramount important role in the final morphology of the as-grown CNFs. For instance, the two-dimensional Ni catalyst plates would lead to the formation of double helical flat CNFs, whereas the diamond-shaped Ni catalyst particles always led to the formation of double helical circular CNFs (**Figure 9a-c**).<sup>81, 82</sup> It should be noted that an equal number of left and right handedness were always observed, indicating that the as-prepared double helical CNFs exhibited no handedness selectivity. The helical pitches are usually uniform in each individual fiber, but dissimilar among different fibers. It was proposed that the helical organization of an individual CNF can be attributed to the presence of catalytic anisotropy between different crystal faces of one catalyst particle (**Figure 9d**).<sup>84, 85</sup> However, the mechanism for the twisting of two helical CNFs grown oppositely from an individual catalyst particle into a double helix was not well addressed yet.

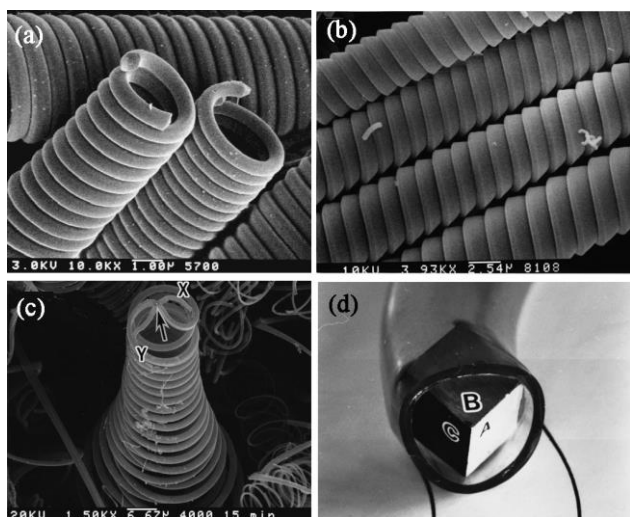


**Figure 9** Representative enlarged views of double helical (a) circular CNFs and (b) flat CNFs; (c) Enlarged view of the tip of the as-grown helical CNF (arrow indicates a Ni catalyst grain); (d) Schematic image of growth mechanism of the helical CNFs.<sup>85</sup> Reprinted with permission from Ref. 85. Copyright 1999 from American Institute of Physics.

Further investigations revealed that the introduction of S into the reaction system can result in the significant anisotropic reactivity of catalyst particles, which led to the double helical morphology of the as-fabricated CNFs much more preferable. For instance, Mukhopadhyay *et al.* found that the addition of thiophene into the acetylene can significantly improve the yield and purity of the double helical CNFs.<sup>86</sup> On the other hand, the Hanus group demonstrated that the growth pattern and surface morphology of

CNFs can be significantly changed upon the modification of polycrystalline Ni catalyst particles by H<sub>2</sub>S, which gave rise to a unique twisted CNFs composed of four intertwined helical strands.<sup>87</sup> This indicated that the direct modification of the catalyst particles by S-containing compounds was also expected to promote the formation of double helical CNFs.

Other carbon precursors (*e.g.* methane and acetone) and other transition metal particles (including Fe, Cu, and their alloys) have also demonstrated to be effective for the growth of double helical CNFs.<sup>88-91</sup> Both the diameter and the yield of the as-obtained double helical CNFs varied a lot. This indicated that the growth of double helical CNFs from the catalytic deposition of carbon sources on metal particles was a general phenomenon. A different kind of catalyst for the catalytic growth of double helical CNFs was reported by Zhang *et al.* They found that the catalytic CVD of acetylene over NiCuMgAl-layered double hydroxides (LDHs), double micro-coiled carbon fibers can be available.<sup>92</sup> However, twist-shaped nanocoiled carbon fibers were obtained when using Mg-free NiCuAl LDHs as the catalyst. The LDHs which consist of positively charged layers and charge-balancing interlayer anions are a class of brucite-like layered materials. Most metal cations, including Mg<sup>2+</sup>, Al<sup>3+</sup>, Fe<sup>3+</sup>, Co<sup>2+</sup>, Ni<sup>2+</sup>, Cu<sup>2+</sup>, and Zn<sup>2+</sup>, can be well arranged into the positive layers of the LDHs with controlled compositions at an atomic level.<sup>76, 93, 94</sup> Therefore, the use of LDHs as the catalyst for the growth of double helical CNFs greatly extended the catalyst family and made the structure of the as-obtained double-helical CNFs much more controllable.

#### 2.1.4.2 Carbon nanotube double helices

Carbon nanotubes (CNTs) have been extensively investigated since their discovery due to their ultrahigh aspect ratio, extraordinary strength and unique electrical properties. The structure and geometry of CNTs play an important role in their properties. Soon after the discovery of CNTs, the presence of single helical CNTs was predicted theoretically by physicists based on the molecular-dynamics simulations involving the pentagons and heptagons in the structure of CNTs.<sup>95, 96</sup> The experimental observation and synthesis of individual helical CNTs have been extensively reported.<sup>7, 79, 97-100</sup>

However, the fabrication of CNTs with double helical configuration was rarely reported until the very recent works carried out by the Wei group that the lamellar transition metal-containing LDHs can effectively catalyze the growth of CNT-array double helices upon the decomposition of carbon sources.<sup>12</sup> After the calcination and reduction of the LDH flakes, catalyst NPs with high density, small size, and extraordinary thermal stability can be produced on both sides of the resulted layered double oxide (LDO) flakes, which will catalyze the synchronous growth of aligned CNTs on both sides of the LDO flakes after the introduction of a carbon source at high temperature (**Figure 10a**).<sup>12, 101</sup> The as-grown aligned CNTs on the opposite sides of the LDOs were then self-organized into a unique double helical morphology. The as-fabricated CNT-array double helices exhibited a closely packed nanostructure with a catalyst flake on the tip, which connected the two helical CNT stands on both sides of the flake (**Figure 10b**). The length of the CNT-array

double helices can be up to tens of micrometers with a diameter of several micrometers, which was controllable depending on the lateral size of the LDH flakes. Further study revealed that the introduction of Mo element into the LDHs would significantly reduce the size of the catalyst NPs embedded on the LDOs while improve their density due to the pinning effect of Mo around metal NPs, which was important for the growth of CNTs with smaller diameter and less wall number.<sup>101</sup> The Mo-containing LDHs were demonstrated to be effective for the fabrication of single-walled CNT (SWCNT)-array double helices (**Figure 10c-e**).<sup>101-103</sup> As a result, the wall number of CNTs in the as-grown CNT-array double helices can be well controlled using LDHs with different compositions, including SWCNTs<sup>101-103</sup>, double-walled CNTs (DWCNTs),<sup>12</sup> and multi-walled CNTs<sup>12</sup>. Furthermore, it needs to be highlighted that the self-organization of N-doped CNT-array double helices were achieved using the FeMgAl LDH catalyst with the co-feeding of the carbon source ( $C_2H_4$ ) and the nitrogen source ( $CH_3CN$ ) (**Figure 10f**).<sup>104</sup> The as-fabricated N-doped CNT-array double helices were with a length of 10-36  $\mu m$ , a screw pitch of 1-2  $\mu m$ , a CNT diameter of 6-10 nm, and a N-content of 2.59 at.%. It was demonstrated that the co-feeding of  $C_2H_4$  and  $CH_3CN$  was of paramount importance for the successful organization of the N-doped CNT-array double-helix structure. The organization of N-doped CNTs in double helical configuration sees their potential applications in the fields of catalysis, mechanic devices, and electrochemical energy storage.

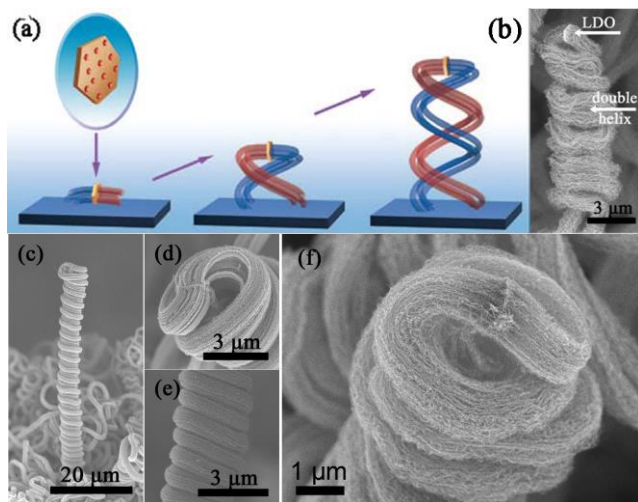


**Figure 10** (a) Scheme showing the formation process of the CNT-array double helix; (b) Scanning electron microscope (SEM) image of a typical double-walled CNT-array double helix;<sup>12</sup> (c) SEM image of an as-grown SWCNT double helix from FeMoMgAl LDH flakes and (d) its top section with a piece of LDO flake, as well as (e) the middle section with the twisted SWCNT strands;<sup>102</sup> (f) SEM images showing a N-doped CNT-array double helix.<sup>104</sup> Reprinted with permission from Ref. 12. Copyright 2010 from Wiley-VCH. Reprinted with permission from Ref. 102. Copyright 2011 from Elsevier. Reprinted with permission from Ref. 104. Copyright 2012 from Elsevier.

The catalytic deposition of CNTs on a lamellar flake with high-density catalyst NPs carried out by the Wei group provided a general method for the fabrication of CNTs with double helical configuration. For instance, the very recent report by Cervantes-Sodi *et al.* demonstrated that CNT-array double helices can also be available using lamellar  $SiO_x$  particles-supported Fe NPs as the catalyst flakes.<sup>105,106</sup> However, it should be noted that it still remains a challenge to synthesize a true CNT double helix in which each backbone is one individual CNT with its own helicity rather than one CNT array.

#### 2.1.4.3 Formation mechanism of CNT double helices

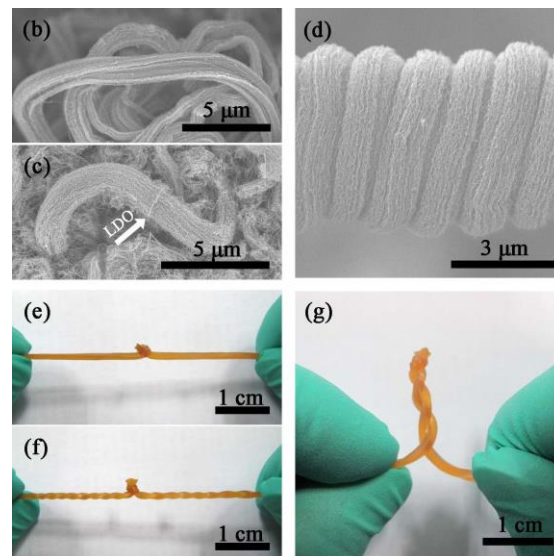
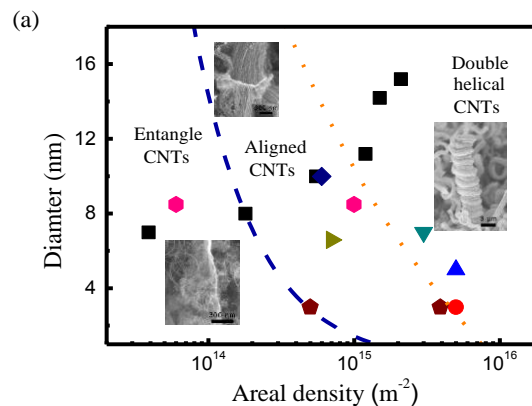


**Figure 11** (a) The phase diagram of CNTs grown on flat/flake substrates with different catalyst NP densities and sizes;<sup>107</sup> SEM image showing (b) a long CNT bundle with obvious rotation, (c) two CNT bundles grown oppositely from a LDO flake with the same right-handed rotation, and (d) the non-rotation of the CNT bundles in the CNT-array double helix; (e-g) Photo images showing evolution process of the self-organization of a twisted rubber band with a node into a double-helical structure.<sup>103</sup> Reprinted with permission from Ref. 103. Copyright 2012 from American Chemical Society. Reprinted with permission from ref. 107. Copyright 2014 from Royal Society of Chemistry.

The investigation of the formation mechanism of the inorganic double helical structure is the prerequisite for the fundamental studies of their controllable synthesis and properties. Detailed investigations have been carried out to address the essentials and the driven force for the formation of the CNT-array double helices.

First, it was demonstrated that the size and areal density of the catalyst NPs on LDO flakes played an important role in the formation of CNT-array double helices (**Figure 11a**).<sup>107</sup> A spectrum of FeMgAl LDHs with different Fe contents was synthesized to obtain ultra-dispersed catalyst NPs with controllable size and areal density. It was found that when the areal density of catalyst NPs was low, only randomly entangled CNTs were obtained. With the increase of the areal density, short aligned CNTs became available.<sup>107</sup> This can be attributed from the synchronous growth of CNTs from the high-density catalyst NPs. With the further increase of the areal density of the catalyst NPs, it was noticed that the as-grown aligned CNTs were self-organized into a double helical structure. Furthermore, the smaller the size of the catalyst NPs was, the higher areal density would be required for the morphology transformation.

Through directly observing their formation process from individual LDH flake under SEM, the space confinement and rotation stress induced self-organization mechanism of the CNT-array double helices (**Figure 11b-g**) has been proposed.<sup>103</sup> It was found that the space confinement was the most important extrinsic factor for the formation of CNT-array double helical structure. Synchronous growth of CNT arrays oppositely from LDH flakes with space confinement on both sides at the same time was considered to be essential for the growth CNT-array double helices, which provided a propulsive force to lift up the LDO flakes. Coiling of the two aligned CNTs on both sides of the LDO flake then preceded with self-organization, tending to the most stable morphology in order to release their internal rotation stress, leading to the formation of double-helix structure (**Figure 7a-c**).

A rubber band with a node was taken as an example to further demonstrate such mechanism (**Figure 11e-g**). It was further noticed that the self-organization of two fibers with left-handed self-rotation connected by a node led to the formation of a double-helix structure with two right-handed helices. On the contrast, the self-organization of two fibers with right-handed self-rotation connected by a node led to the formation of a double-helix with two left-handed helices. This indicated that the chirality of the self-organized double helices depended on the self-rotation direction of the two original fibers, which might contribute to the handedness selective synthesis of inorganic double helical structures. The rotation stress-releasing formation mechanism can commendably explain why only catalyst NPs with very high density can induce the formation of CNT-array double helices. It is because that the density of metal NP catalysts plays a key role for the self-assembly of aligned CNTs into double-helix structure due to the fact that internal rotation stress contributed from a large number of growing CNTs should be over a critical value before it can be self released.

The original of the internal rotation stress of the as-grown aligned CNTs on both sides of the LDO flakes is disputable. On one hand, it was proposed to be resulted by the fact that the intrinsic rotation of individual CNTs was impeded by neighboring CNTs.<sup>103, 108</sup> On the other hand, theoretical calculations based on an adhesion-based model demonstrated that the interfacial adhesion among the CNTs could be the driven force for the self-rotation of the as-grown aligned CNTs.<sup>109</sup> However, the rotation stress-releasing mechanism can still be used to explain the self-organization of other kinds of double helical structures, such as the self-assembly of the two helical CNFs grown oppositely from a catalyst particle into a double-helix structure<sup>81, 86</sup> and the formation of Ag-Au double helical nanowires<sup>13</sup>. Therefore, it is believed that this rotation stress-releasing mechanism could provide a basic principle for the fabrication of inorganic double-helical structures.

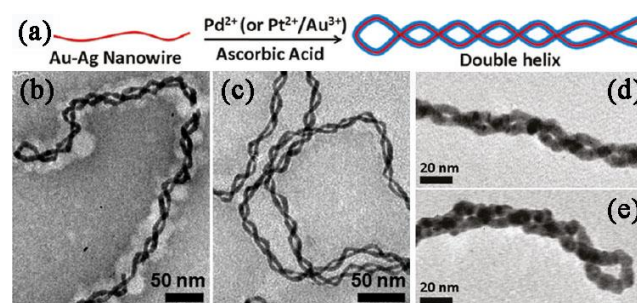


**Figure 12** (a) Schematics illustrating the formation of double helix by growing a metal layer on Au-Ag alloy nanowire; TEM images of the (b, c) (Au-Ag)@Pd and (d, e) (Au-Ag)@Au double helices.<sup>13</sup> Reprinted with permission from Ref. 13. Copyright 2011 from American Chemical Society.

## 2.2 Top-down strategy

### 2.2.1 Nanoscale chemical modification

As mentioned previously, the external stimuli plays an important role in the successful self-organization of double helical structures. Therefore, it is expected that the changing of the external environment or the surface properties of the previously prepared fibers could lead to their organization into double helical structures. Maeda *et al.* synthesized two complementary homopolymers of chiral amidines and achiral carboxylic acids with *m*-terphenyl-based backbones. Upon mixing in THF, it was found that the homopolymer fibers assembled into a preferred-handed double helix through interstrand amidinium-carboxylate salt bridges.<sup>110</sup> However, only an interpolymer complex with an imperfect double helical structure containing a randomly hybridized cross-linked structure was formed when mixed in less polar solvents, such as chloroform. It was interesting to find that such primary complex could be rearranged into the fully double helical structure by treatment with a strong acid followed by neutralization with an amine. However, the basic principle of this morphology transformation was not well addressed yet. With the pre-synthesized Au-Ag alloy nanowires with the helical arrangement of Au and Ag atoms, Want *et al.* reported the unprecedented chiral transformation of the single Au-Ag nanowires to a double-helix structure upon growth of an additional metal layer (Pd, Pt, or Au) by a chemical method in solution (**Figure 12**).<sup>13</sup> TEM

images showed that the helices were made from the self-winding of a single nanowire, rather than the intertwining of multiple nanowires. It was demonstrated that the rate of metal deposition was a critical factor in inducing the winding of single nanowires into double helical morphologies. The formation of the double helices was proposed to be the consequence of the untwisting of the single nanowires due to their tendency to release the strain originated from the coating of a metal layer on the Au-Ag alloy nanowires. It is worthy to note that the rotation stress-releasing mechanism discussed in Section 2.1.4.3 can also be invoked herein to explain such a phenomenon.

### 2.2.2 Microscale transformation under capillary force

Capillary force is also considered as an effective driven force for the fabrication of double helical structures since it has been demonstrated that spontaneous helicity can be induced in soft nanopillars under the capillary force. For instance, Pokroy *et al.* carried out the study of immersing a polymer nanopillar array prepared using lithographic methods in liquid and then dried it in air.<sup>111</sup> It was interesting to find that the capillary force induced by the evaporation of the liquid forced the neighboring nanopillars to tilt towards each other, leading to the formation of helical bundles. The parameters of the nanopillar arrays can be tuned to achieve various different helical patterns, and double helical structures can be formed when applying this process onto an array of ordered helical pairs. One of the most interesting characteristics was that the handedness of the as-fabricated helical bundles can be well controlled through setting the initial tilting direction. Using inorganic materials, the Hart group reported the formation of helically twisted CNT bundles.<sup>112</sup> Vertical CNT cylinders prepared using ring-shaped catalysts were first immersed into liquid. The CNTs within the individual cylinders formed twisted helices under the generated capillary force upon evaporation of the liquid in order to maximize their mutual stacking (**Figure 13a**). A single handedness can also be obtained by well controlling the pattern of

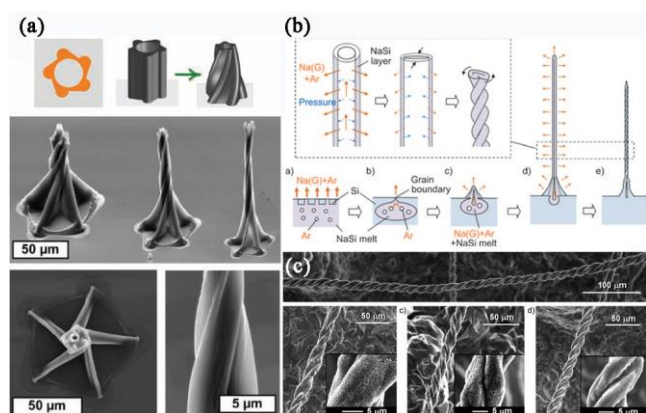


**Figure 13** (a) CNT micro-helices with deterministic handedness and pitch made by capillary forming,<sup>112</sup> (b) Proposed formation mechanism of double-helical Si microtubes; (c) SEM micrographs of the double-helical Si microtubes prepared by heating the Zintl compound NaSi.<sup>11</sup> Reprinted with permission from Ref. 11 and 112. Copyright 2010 from Wiley-VCH.

the ring-shaped catalyst. However, the formation of double helical CNT bundles was not reported in this work. A rather unique work on the fabrication of double helical silicon microtubes was reported recently by Morito *et al.*<sup>11</sup> Typically, a disk of compact Zintl compound NaSi powder was used as the starting material, which was heated to 800 °C in a temperature-gradient reactor and kept for 12 h to induce the evaporation of Na from the NaSi disk. As a result, a large number of double helical Si microtubes with a diameter of 10–50 μm and a length of several hundred micrometers to 2.5 mm were obtained on the disk surface (**Figure 13b and c**). It was proposed that the Si microtubes were extruded from the melted NaSi powder because of the trapping of the evaporated Na and Ar gas (**Figure 13b**). The formation of the double helical Si microtubes was caused by the leaking of the evaporated Na and Ar gas, which probably generated the capillary forces to induce the helical configuration.

### 2.2.3 Macroscopic processing

The development of nanotechnology and techniques has allowed much better manipulation of micro/nanomaterials to control their morphologies. The Cao group succeeded in the fabrication of a high twisted CNT yarn-derived double-helix structure by a conventional twist-spinning process. Typically, a straight CNT yarn was fabricated firstly using a CNT film with two ends fixed on an electric motor and a metal block fixer. Then, the straight yarn was spun into a helical yarn by continued over-twisting, which was transformed into a double-helix configuration through applying a small force to the middle point of the helical CNT yarn. The as-fabricated CNT double helix consisting of two single-helical CNT yarn segments is with its diameter and pitch controllable in the range of tens of micrometers.

In addition, direct laser writing (DLW) is one of the mostly used techniques to create different kinds of three-dimensional polymer structures. A regular array of helical air voids in the polymer structure *via* an approach based on DLW into a positive-tone photoresist was fabricated by Gansel *et al.*, which was then used as the template for the fabrication of helical Au arrays.<sup>113</sup> It should be noted that only those regions that are sufficiently exposed by light are removed in the development process for positive-tone photoresists. On the other hand, only the sufficiently exposed regions remain after the development process for negative-tone photoresists.<sup>114</sup> Therefore, the DLW method could be expected to be effective for creating the double helical organic nanostructures. Besides, other macroscopic techniques that allows precise micro/nanoscale processing, such as reactive ion etching and especially the newly developed 3D printing techniques, could also be expected for the fabrication of double helical micro/nanostructures with much more precisely controlled morphology.

## 3. Promising properties of double helical structures

Materials with double helical structures could be with promising and excellent mechanical, electromagnetic, and optical properties. However, characterizing or measuring the properties of the double helical structures has always been a great challenge due to their micro/nanoscale size, which makes it difficult to observe and manipulate the double helices to measure their properties. Besides,

in the as-established strategies for the fabrication of double helical structures, there are always large quantities of by-products, such as single helical structures and non-coiled one-dimensional fibers. The preparation of double helical structures with high purity and selectivity still remains a challenge, which also hinders the investigation on their properties. Therefore, studies of the specific double helicity-induced property for micro/nanomaterials are still in exploration stage.

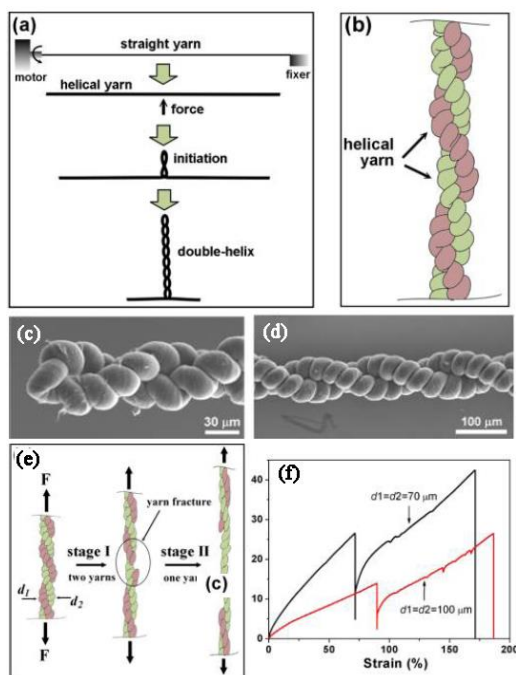


**Figure 14** (a) Illustration of a spinning process starting from a straight CNT yarn; (b) Illustration of the double-helix CNT yarns consisting of two single-helical yarns twisted together; (c) Close view of the top end which is the initiation position for the double-helix CNT yarns. (d) SEM image of the middle section showing two helical yarns twisted tightly; (e) Illustration of the tensile testing process including two stages where two yarns sustain the force ( $F$ ) together during stage I until one of the yarns fractures, and after that the remaining yarn is stretched during stage II until complete fracture; (f) The stress-strain curves by the load divided by the sum of cross-sectional area of the two yarns for stage I, and the load divided by the cross-sectional area of the remaining yarn for stage II.<sup>15</sup> Reprinted with permission from Ref. 15. Copyright 2013 from American Chemical Society.

The most promising property for the double helical materials is their mechanical property due to their similarities with springs. Some *in situ* manipulators, such as atomic force microscopy and SEM, have been employed to investigate the mechanical properties of the micro/nanoscale double helical structures. Early in 1990s, the Motojima group have found that the double helical CNFs can be extended and contracted by about three to fifteen times of their original length, and then recovered.<sup>82</sup> The self-organized CNT-array double helices can also be stretched, which were able to return to their original form if the stretching was performed under the limited

value of elastic deformation.<sup>12, 102</sup> The quantitative characterization of the mechanical properties of a highly twisted CNT yarns with double-helix structure was carried out by the Cao group (Figure 14a-d).<sup>15</sup> It was demonstrated that the as-fabricated multifunctional double-helix CNT yarns were elastic within a certain strain range ( $\epsilon < 20\%$ ), and could recover to initial morphology without permanent deformation. Cyclic stress-strain curves measured on the double-helix yarns at a series of increasing maximum strains showed linear loading and unloading curves with a hysteresis loop and similar modulus during the repeated loading. During the mechanical tests, one of the CNT yarns broke early under tension due to the highly twisted state, however, the second CNT yarn produced much larger tensile strain and significantly prolonged the process until ultimate fracture (Figure 14e and f). In most cases, the first yarn broke at a relatively small strain ( $\epsilon < 100\%$ ) while the second yarn broke at a much large strain ( $\epsilon < 150\%$ ). The overall toughnesses of the two stages were calculated to be 7-15 and 17-26 J/g, respectively.

It is well-known that when passing an electrical current through a conductive helix, magnetic field will be generated, which makes the double helical structures a starting point for the study of electromagnetic phenomena at the micro/nanoscale. Up to now, several conductive helices, including double helical CNFs, CNT arrays, and Au-Ag nanowires, have been strongly considered.<sup>12, 13, 16</sup> These conductive helices can be considered as solenoids and excellent electromagnetic properties at micro/nanoscale can be expected. However, the experimental investigation on the induced magnetic field is difficult due to the measurement of magnetic properties at the micro/nanoscale still faces great challenges. For instance, Zhang *et al.* applied parallel and inverse current to each “backbone” of the CNT-array double helices inside a SEM at room temperature by using a nanoprobe system.<sup>12</sup> Current densities as high as  $2.9 \times 10^7 \text{ A cm}^{-2}$  were loaded onto the CNT arrays. However, the magnetic field was estimated to be about  $1 \times 10^{-4} \text{ T}$  (current: 1 mA), which was too weak to induce the movement of CNT stands in the double helix. On the other hand, it was found that the helical arrangement of conductive materials could significantly influence their electrical properties. Motojima *et al.* reported that the electrical resistivity, inductance, and capacitance of double helical CNFs were all influenced by the motions of extension and contraction, which made them a promising candidate for tactile sensors.<sup>16</sup> In addition, Shang *et al.* demonstrated that the as-fabricated conductive double-helix CNT yarns showed simultaneous and reversible resistance change in response to applied stains or stresses, light illumination, and environmental temperature, indicating the promising applications of the double-helix structures as strain sensors, photo detectors, and thermocouple-like devices.<sup>15</sup> The use of twisted CNT yarns as a wire device that can be easily woven into textiles or other structures to provide active sites for charge storage was recently explored by Peng's group.<sup>17</sup> It is highly expected that double helical nanocarbon based/derived structures offer highly electrochemical activity for microsupercapacitors, microbatteries, as well as micro-solar cells.

Because the helical nanostructures are always uniaxial which associates them with birefringence, the responses to light can relate

to both reflection and absorption.<sup>18, 19</sup> Good light absorption properties can be expected for helical nanostructures built up with conductive materials. For example, Tang *et al.* reported the good absorption properties of microwave for double helical CNFs.<sup>115</sup> They supposed that such good absorption property was ascribed to dielectric rather than magnetic loss by measuring the permeability, permittivity, and loss tangent spectra. It was also reported that composites containing the double helical CNFs and paraffin exhibited very strong microwave absorption performance in a frequency range of 2 to 18 GHz. It indicated the possibility of wideband absorption when a double-layered absorber made of two composites of different thickness or double-helical CNF content was utilized. This also facilitates the potential applications of double helical structures in stealth materials to prevent radar from microwave radiation disturbances.

#### 4. Conclusions and outlook

The recent research progress on the fabrication of materials with a double helical morphology has been reviewed. A variety of different strategies and synthetic methods have been explored to fabricate double helical structures, including both the “bottom-up” and “top-down” strategies. The self-organization of double helical organic micro/nanomaterials has been well achieved through the self-assembly of amphiphilic molecules. The template assembly of inorganic molecules and NPs using the double helical organic structures as the templates can lead to well-defined inorganic double helical structures. However, the template-free synthesis process is much more attractive due to the fact that it always involves the self-organization of atoms and crystal growth, which give rises to double helical materials with much better crystallization, purity, and better properties. Solution based reactions that involve the staggered stacking of building blocks under the anisotropic growth mode can also lead to the formation of inorganic double helical structures. Both the theoretical simulation and experimental results revealed that the self-organization of nanoscale fibers or even atoms under the physical confinement effect will lead to the formation of a double helical configuration to achieve their most stable state. The catalytic deposition of the self-organized double helical carbon fibers and CNTs under anisotropic growth mode has been extensively investigated. The proposed rotation stress-releasing formation mechanism can not only be used to the explain the formation process of CNT-array double helices, but also work for other kinds of inorganic double helical structures in which the two helical backbones are connected at a node. For the “top-down” strategy, multiscale methods, such as the nanoscale chemical modification, microscale self-transformation, and macroscopic processing techniques, have been explored to induce the double-helical morphology for micro/nanomaterials.

It has to be admitted that the investigations on the preparation of double helices are still at the preliminary stage. Some issues are still to be addressed before the practical applications of double helical materials, such as the high yield and high purity synthesis of double helical structures, how to differentiate left handedness from right handedness as nature and organic materials did, and better control

over the pitches of double helical structures. These structure features are directly linked to properties and potential applications of double helical structures. The well-controlled and large scale synthesis of double helical structures is the first step towards their practical applications. The selective preparation of organic double helical structures with single handedness can be achieved using chiral building blocks, which are able to direct the template growth of inorganic replicates with selective handedness. However, the basic principle for the handedness selective or even separation for self-assembled inorganic double helical materials is still to be further understood.

There are many candidates as the building blocks for the double helical nanostructures. The DNA, copolymers, chiral dimer, as well as nanocarbon (*e.g.* CNTs, graphene fibers, carbon-inorganic hybrids) are promising single helices. The property of the single helices can be well tuned by the composition and structure, which brings novel potential applications for advanced energy storage, environmental protection, healthcare, and information technology. The matching between the two congruent single helices in the double helical structure provides possibility to record and replicate information, which is a potential DNA-like synthetic nanostructures.

Due to the difficulty in achieving double helical materials with high purity and handling them at the micro/nanoscale, very few studies on the properties of double helical structure are able to be carried out up to now. Such investigations are the prerequisite and can direct the practical use of the inorganic double helices. Techniques for handling and manipulating the micro/nanostructured double helical materials are to be further developed. In addition, more efforts are to be devoted on the integration and regularity of double helices due to their ability to bridge the nanostructures to meso- or macro-properties. Promising properties of the double helical structures towards their applications in the fields of mechanical and electromagnetic devices, catalysis, information storage, and intelligent drug delivery etc. are to be further investigated.

Up to now, the family of the double helical materials is still limited, and more micro/nanomaterials in double helical configuration are emerging. For instance, Ivanov *et al.* theoretically predicted the existence of double-helix structures in the series of  $\text{Li}_x\text{P}_x$  ( $x = 5-9$ ) cluster and in an infinite  $\text{LiP}$  chain.<sup>116</sup> The nature of bonding in these double helices was also theoretically analyzed to find out the origin of the stabilization of such  $\text{Li}_x\text{P}_x$  inorganic double helices.<sup>117</sup> It was surprising to discover the double helical structures in such rather simple species consisting of lithium and phosphorus. Experimental synthesis of this simple double-helix inorganic material is to be carried out. In general, more strategies, formation mechanisms, and even theoretical studies are required to further understand and direct the fabrication to enlarge the family of double helical structures.

#### Acknowledgements

This work was supported by National Basic Research Program of China (973 Program, 2011CB932602) and Natural Scientific Foundation of China (No. 21306102).

## Notes and references

\* Beijing Key Laboratory of Green Chemical Reaction Engineering and Technology, Department of Chemical Engineering, Tsinghua University, Beijing 100084, P. R. China. E-mail: zhang-qiang@mails.tsinghua.edu.cn (Q. Zhang); wf-dce@tsinghua.edu.cn (F. Wei)

- 1 M. Albrecht, *Chem. Rev.*, 2001, **101**, 3457-3498, and references therein.
- 2 D. S. Su, *Angew. Chem. Int. Ed.*, 2011, **50**, 4747-4750.
- 3 M. Yang and N. A. Kotov, *J. Mater. Chem.*, 2011, **21**, 6775-6792, and references therein.
- 4 C. C. Lee, C. Grenier, E. W. Meijer, and A. P. H. J. Schenning, *Chem. Soc. Rev.*, 2009, **38**, 671-683.
- 5 Y. Wang, J. Xu, Y. W. Wang, and H. Y. Chen, *Chem. Soc. Rev.*, 2012, **42**, 2930-2962, and references therein.
- 6 H. Imai and Y. Oaki, *Angew. Chem. Int. Ed.*, 2004, **43**, 1363-1368.
- 7 M. J. Hanus and A. I. Harris, *J. Nanosci. Nanotechnol.*, 2010, **10**, 2261-2283.
- 8 Y. Han, L. Zhao, and J. Y. Ying, *Adv. Mater.*, 2007, **19**, 2454-2459.
- 9 S. Yang, L. Zhao, C. Yu, X. Zhou, J. Tang, P. Yuan, D. Chen, and D. Zhao, *J. Am. Chem. Soc.*, 2006, **128**, 10460-10466.
- 10 S. Jin, M. J. Bierman, and S. A. Morin, *J. Phys. Chem. Lett.*, 2010, **1**, 1472-1480.
- 11 H. Morito and H. Yamane, *Angew. Chem. Int. Ed.*, 2010, **49**, 3638-3641.
- 12 Q. Zhang, M. Q. Zhao, D. M. Tang, F. Li, J. Q. Huang, B. L. Liu, W. C. Zhu, Y. H. Zhang, and F. Wei, *Angew. Chem. Int. Ed.*, 2010, **49**, 3642-3645.
- 13 Y. Wang, Q. Wang, H. Sun, W. Zhang, G. Chen, Y. Wang, X. Shen, Y. Han, X. Lu, and H. Chen, *J. Am. Chem. Soc.*, 2011, **133**, 20060-20063.
- 14 L. Jun, X. Zhang, Z. Yingjiu, C. Xihua, and Z. Jing, *Mater. Res. Bull.*, 2003, **38**, 261-267.
- 15 Y. Shang, Y. Li, X. He, S. Du, L. Zhang, E. Shi, S. Wu, Z. Li, P. Li, J. Wei, K. Wang, H. Zhu, D. Wu, and A. Cao, *ACS Nano*, 2013, **7**, 1446-1453.
- 16 S. Motojima, X. Chen, S. Yang, and M. Hasegawa, *Diam. Relat. Mater.*, 2004, **13**, 1989-1992.
- 17 J. Ren, L. Li, C. Chen, X. L. Chen, Z. B. Cai, L. B. Qiu, Y. G. Wang, X. R. Zhu, and H. S. Peng, *Adv. Mater.*, 2013, **25**, 1155-1159.
- 18 K. Robbie and M. J. Brett, *J. Vac. Sci. Technol. A*, 1997, **15**, 1460-1465.
- 19 K. Robbie, J. C. Sit, and M. J. Brett, *J. Vac. Sci. Technol. B*, 1998, **16**, 1115-1122.
- 20 J. Dupont, G. Liu, K.-i. Niihara, R. Kimoto, and H. Jinnai, *Angew. Chem. Int. Ed.*, 2009, **48**, 6144-6147.
- 21 Y. Yan, Y. Lin, Y. Qiao, and J. Huang, *Soft Matter*, 2011, **7**, 6385-6398.
- 22 R.-M. Ho, Y.-W. Chiang, S.-C. Lin, and C.-K. Chen, *Prog. Polym. Sci.*, 2011, **36**, 376-453.
- 23 H. Yanagawa, Y. Ogawa, H. Furuta, and K. Tsuno, *J. Am. Chem. Soc.*, 1989, **111**, 4567-4570.
- 24 R. Oda, I. Huc, and S. J. Candau, *Angew. Chem. Int. Ed.*, 1998, **37**, 2689-2691.
- 25 Y. Lin, Y. Qiao, C. Gao, P. Tang, Y. Liu, Z. Li, Y. Yan, and J. Huang, *Chem. Mater.*, 2010, **22**, 6711-6717.
- 26 Y. Lin, A. Wang, Y. Qiao, C. Gao, M. Drechsler, J. Ye, Y. Yan, and J. Huang, *Soft Matter*, 2010, **6**, 2031-2036.
- 27 S. Yagai, M. Yamauchi, A. Kobayashi, T. Karatsu, A. Kitamura, T. Ohba, and Y. Kikkawa, *J. Am. Chem. Soc.*, 2012, **134**, 18205-18208.
- 28 S. Zhong, H. Cui, Z. Chen, K. L. Wooley, and D. J. Pochan, *Soft Matter*, 2008, **4**, 90-93.
- 29 E. Lee, B. Hammer, J.-K. Kim, Z. Page, T. Emrick, and R. C. Hayward, *J. Am. Chem. Soc.*, 2011, **133**, 10390-10393.
- 30 H. Dou, G. Liu, J. Dupont, and L. Hong, *Soft Matter*, 2010, **6**, 4214-4222.
- 31 S. Hong, T. Higuchi, H. Sugimori, T. Kaneko, V. Abetz, A. Takahara, and H. Jinnai, *Polym. J.*, 2012, **44**, 567-572.
- 32 H. Jinnai, T. Kaneko, K. Matsunaga, C. Abetz, and V. Abetz, *Soft Matter*, 2009, **5**, 2042-2046.
- 33 H. Qiu and S. Che, *Chem. Soc. Rev.*, 2011, **40**, 1259-1268.
- 34 S. Che, Z. Liu, T. Ohsuna, K. Sakamoto, O. Terasaki, and T. Tatsumi, *Nature*, 2004, **429**, 281-284.
- 35 H. Qiu, S. Wang, W. Zhang, K. Sakamoto, O. Terasaki, Y. Inoue, and S. Che, *J. Phys. Chem. C*, 2008, **112**, 1871-1877.
- 36 H. Jin, H. Qiu, Y. Sakamoto, P. Shu, O. Terasaki, and S. Che, *Chem. Eur. J.*, 2008, **14**, 6413-6420.
- 37 Y. Zhou and T. Shimizu, *Chem. Mater.*, 2008, **20**, 625-633.
- 38 X. W. Wu, H. Y. Jin, Z. Liu, T. Ohsuna, O. Terasaki, K. Sakamoto, and S. N. Che, *Chem. Mater.*, 2006, **18**, 241-243.
- 39 J. H. Jung, K. Yoshida, and T. Shimizu, *Langmuir*, 2002, **18**, 8724-8727.
- 40 Y. G. Yang, M. Suzuki, S. Owa, H. Shirai, and K. Hanabusa, *J. Mater. Chem.*, 2006, **16**, 1644-1650.
- 41 K. Sugiyasu, S. Tamaru, M. Takeuchi, D. Berthier, I. Huc, R. Oda, and S. Shinkai, *Chem. Commun.*, 2002, 1212-1213.
- 42 Y. G. Yang, M. Suzuki, S. Owa, H. Shirai, and K. Hanabusa, *Chem. Commun.*, 2005, 4462-4464.
- 43 V. Soghomonian, Q. Chen, R. C. Haushalter, J. Zubieta, and C. J. Oconnor, *Science*, 1993, **259**, 1596-1599.
- 44 C.-L. Chen and N. L. Rosi, *Angew. Chem. Int. Ed.*, 2010, **49**, 1924-1942.
- 45 S. Guha, M. G. B. Drew, and A. Banerjee, *Small*, 2008, **4**, 1993-2005.
- 46 K. J. C. van Bommel, A. Friggeri, and S. Shinkai, *Angew. Chem. Int. Ed.*, 2003, **42**, 980-999.
- 47 A. Kuzyk, R. Schreiber, Z. Fan, G. Pardatscher, E.-M. Roller, A. Hoeggele, F. C. Simmel, A. O. Govorov, and T. Liedl, *Nature*, 2012, **483**, 311-314.
- 48 J. Sharma, R. Chhabra, A. Cheng, J. Brownell, Y. Liu, and H. Yan, *Science*, 2009, **323**, 112-116.
- 49 H. Kuang, W. Ma, L. Xu, L. Wang, and C. Xu, *Accounts. Chem. Res.*, 2013, **46**, 2341-2354, and references therein.
- 50 L. Xu, W. Ma, L. Wang, C. Xu, H. Kuang, and N. A. Kotov, *Chem. Soc. Rev.*, 2013, **42**, 3114-3126, and references therein.
- 51 W. Ma, H. Kuang, L. Xu, L. Ding, C. Xu, L. Wang, and N. A. Kotov, *Nat. Commun.*, 2013, **4**, 2689.
- 52 W. Ma, H. Kuang, L. Wang, L. Xu, W.-S. Chang, H. Zhang, M. Sun, Y. Zhu, Y. Zhao, L. Liu, C. Xu, S. Link, and N. A. Kotov, *Sci. Rep.*, 2013, **3**, 1934.
- 53 C.-L. Chen, P. Zhang, and N. L. Rosi, *J. Am. Chem. Soc.*, 2008, **130**, 13555-13557.
- 54 C. Song, M. G. Blaber, G. Zhao, P. Zhang, H. C. Fry, G. C. Schatz, and N. L. Rosi, *Nano Lett.*, 2013, **13**, 3256-3261.
- 55 A. M. Seddon, H. M. Patel, S. L. Burkett, and S. Mann, *Angew. Chem. Int. Ed.*, 2002, **41**, 2988-2991.

- 56 Y. M. Lvov, R. R. Price, J. V. Selinger, A. Singh, M. S. Spector, and J. M. Schnur, *Langmuir*, 2000, **16**, 5932-5935.
- 57 Y. Zhou, Q. M. Ji, M. Masuda, S. Kamiya, and T. Shimizu, *Chem. Mater.*, 2006, **18**, 403-406.
- 58 R. R. Price, W. J. Dressick, and A. Singh, *J. Am. Chem. Soc.*, 2003, **125**, 11259-11263.
- 59 E. D. Sone, E. R. Zubarev, and S. I. Stupp, *Angew. Chem. Int. Ed.*, 2002, **41**, 1705-1709.
- 60 E. D. Sone, E. R. Zubarev, and S. I. Stupp, *Small*, 2005, **1**, 694-697.
- 61 J. H. Jung, Y. Ono, K. Hanabusa, and S. Shinkai, *J. Am. Chem. Soc.*, 2000, **122**, 5008-5009.
- 62 J. H. Jung, H. Kobayashi, M. Masuda, T. Shimizu, and S. Shinkai, *J. Am. Chem. Soc.*, 2001, **123**, 8785-8789.
- 63 J. H. Jung, Y. Ono, and S. Shinkai, *Chem. Eur. J.*, 2000, **6**, 4552-4557.
- 64 J. H. Jung, S. H. Lee, J. S. Yoo, K. Yoshida, T. Shimizu, and S. Shinkai, *Chem. Eur. J.*, 2003, **9**, 5307-5313.
- 65 Y. Qin, Y. Kim, L. Zhang, S.-M. Lee, R. B. Yang, A. Pan, K. Mathwig, M. Alexe, U. Goesele, and M. Knez, *Small*, 2010, **6**, 910-914.
- 66 H. Ogiwara, M. Sadakane, Y. Nodasaka, and W. Ueda, *Chem. Mater.*, 2006, **18**, 4981-4983.
- 67 S. H. Yu, H. Colfen, K. Tauer, and M. Antonietti, *Nat. Mater.*, 2005, **4**, 51-U55.
- 68 Y. Oaki and H. Imai, *Langmuir*, 2005, **21**, 863-869.
- 69 Y. Oaki and H. Imai, *J. Am. Chem. Soc.*, 2004, **126**, 9271-9275.
- 70 K. S. Cho, D. V. Talapin, W. Gaschler, and C. B. Murray, *J. Am. Chem. Soc.*, 2005, **127**, 7140-7147.
- 71 J.-H. Zhu, S.-H. Yu, A.-W. Xu, and H. Coelfen, *Chem. Commun.*, 2009, 1106-1108.
- 72 Y. Y. Wu, G. S. Cheng, K. Katsov, S. W. Sides, J. F. Wang, J. Tang, G. H. Fredrickson, M. Moskovits, and G. D. Stucky, *Nat. Mater.*, 2004, **3**, 816-822.
- 73 C. Lv, Q. Xue, M. Shan, N. Jing, C. Ling, X. Zhou, Z. Jiao, W. Xing, and Z. Yan, *Nanoscale*, 2013, **5**, 4191-4199.
- 74 T. Fujimori, R. B. dos Santos, T. Hayashi, M. Endo, K. Kaneko, and D. Tomanek, *ACS Nano*, 2013, **7**, 5607-5613.
- 75 T. W. Chamberlain, J. Biskupek, G. A. Rance, A. Chuvilin, T. J. Alexander, E. Bichoutskaia, U. Kaiser, and A. N. Khlobystov, *ACS Nano*, 2012, **6**, 3943-3953.
- 76 M. Q. Zhao, Q. Zhang, J. Q. Huang, and F. Wei, *Adv. Funct. Mater.*, 2012, **22**, 675-694.
- 77 L. Mleczko and G. Lolli, *Angew. Chem. Int. Ed.*, 2013, **52**, 9372-9387.
- 78 Q. Zhang, J. Q. Huang, W. Z. Qian, Y. Y. Zhang, and F. Wei, *Small*, 2013, **9**, 1237-1265, and references therein.
- 79 J. Q. Huang, Q. Zhang, and F. Wei, *Prog. Chem.*, 2009, **21**, 637-643, and references therein.
- 80 R. T. K. Baker, P. S. Harris, and S. Terry, *Nature*, 1975, **253**, 37-39.
- 81 S. Motojima, M. Kawaguchi, K. Nozaki, and H. Iwanaga, *Carbon*, 1991, **29**, 379-385.
- 82 S. Motojima, M. Kawaguchi, K. Nozaki, and H. Iwanaga, *Appl. Phys. Lett.*, 1990, **56**, 321-323.
- 83 S. M. Yang, X. Q. Chen, and S. Motojima, *Chem. Vapor Depos.*, 2004, **10**, 97-102.
- 84 X. Q. Chen, T. Saito, M. Kusunoki, and S. Motojima, *J. Mater. Res.*, 1999, **14**, 4329-4336.
- 85 S. Motojima and Q. Q. Chen, *J. Appl. Phys.*, 1999, **85**, 3919-3921.
- 86 K. Mukhopadhyay, K. Ram, D. Lal, G. N. Mathur, and K. U. B. Rao, *Carbon*, 2005, **43**, 2400-2402.
- 87 M. J. Hanus and A. T. Harris, *Carbon*, 2010, **48**, 2989-2992.
- 88 S. Yang, X. Chen, M. Kusunoki, K. Yamamoto, H. Iwanaga, and S. Motojima, *Carbon*, 2005, **43**, 916-922.
- 89 Y. Qin, Z. K. Zhang, and Z. L. Cui, *Carbon*, 2003, **41**, 3072-3074.
- 90 Y. Qin, Z. K. Zhang, and Z. L. Cui, *Carbon*, 2004, **42**, 1917-1922.
- 91 X. Q. Chen, S. Motojima, and H. Iwanaga, *Carbon*, 1999, **37**, 1825-1831.
- 92 L. Zhang and F. Li, *Electrochim. Acta*, 2010, **55**, 6695-6702.
- 93 Q. Wang and D. O'Hare, *Chem. Rev.*, 2012, **112**, 4124-4155.
- 94 S. He, Z. An, M. Wei, D. G. Evans, and X. Duan, *Chem. Commun.*, 2013, **49**, 5912-5920.
- 95 B. I. Dunlap, *Phys. Rev. B*, 1992, **46**, 1933-1936.
- 96 S. Ihara, S. Itoh, and J. Kitakami, *Phys. Rev. B*, 1993, **48**, 5643-5647.
- 97 V. Bajpai, L. M. Dai, and T. Ohashi, *J. Am. Chem. Soc.*, 2004, **126**, 5070-5071.
- 98 J. Liu, S. Webster, and D. L. Carroll, *Appl. Phys. Lett.*, 2006, **88**.
- 99 S. Amelinckx, X. B. Zhang, D. Bernaerts, X. F. Zhang, V. Ivanov, and J. B. Nagy, *Science*, 1994, **265**, 635-639.
- 100 X. S. Qi, W. Zhong, X. J. Yao, H. Zhang, Q. Ding, Q. Wu, Y. Deng, C. T. Au, and Y. W. Du, *Carbon*, 2012, **50**, 646-658.
- 101 M. Q. Zhao, Q. Zhang, W. Zhang, J. Q. Huang, Y. Zhang, D. S. Su, and F. Wei, *J. Am. Chem. Soc.*, 2010, **132**, 14739-14741.
- 102 M. Q. Zhao, J. Q. Huang, Q. Zhang, J. Q. Nie, and F. Wei, *Carbon*, 2011, **49**, 2148-2152.
- 103 M. Q. Zhao, Q. Zhang, G. L. Tian, J. Q. Huang, and F. Wei, *ACS Nano*, 2012, **6**, 4520-4529.
- 104 G. L. Tian, M. Q. Zhao, Q. Zhang, J. Q. Huang, and F. Wei, *Carbon*, 2012, **50**, 5323-5330.
- 105 F. Cervantes-Sodi, J. J. Vilatela, J. A. Jimenez-Rodriguez, L. G. Reyes-Gutierrez, S. Rosas-Melendez, A. Iniguez-Rabago, M. Ballesteros-Villarreal, E. Palacios, G. Reiband, and M. Terrones, *Carbon*, 2012, **50**, 3688-3693.
- 106 F. Cervantes-Sodi, A. Iniguez-Rabago, S. Rosas-Melendez, M. Ballesteros-Villarreal, J. J. Vilatela, L. G. Reyes-Gutierrez, E. Palacios, M. Terrones, and J. A. Jimenez-Rodriguez, *Phys. Status Solidi B*, 2012, **249**, 2382-2385.
- 107 G. L. Tian, M. Q. Zhao, B. S. Zhang, Q. Zhang, W. Zhang, J. Q. Huang, T. C. Chen, W. Z. Qian, D. S. Su, and F. Wei, *J. Mater. Chem. A*, 2014, **2**, 1686-1696.
- 108 F. Ding, A. R. Harutyunyan, and B. I. Yakobson, *Proc. Natl. Acad. Sci. U. S. A.*, 2009, **106**, 2506-2509.
- 109 X. Y. Ji, M. Q. Zhao, F. Wei, and X. Q. Feng, *Appl. Phys. Lett.*, 2012, **100**, 263104.
- 110 T. Maeda, Y. Furusho, S.-I. Sakurai, J. Kumaki, K. Okoshi, and E. Yashima, *J. Am. Chem. Soc.*, 2008, **130**, 7938-7945.
- 111 B. Pokroy, S. H. Kang, L. Mahadevan, and J. Aizenberg, *Science*, 2009, **323**, 237-240.
- 112 M. De Volder, S. H. Tawfick, S. J. Park, D. Copic, Z. Zhao, W. Lu, and A. J. Hart, *Adv. Mater.*, 2010, **22**, 4384-4389.
- 113 J. K. Gansel, M. Thiel, M. S. Rill, M. Decker, K. Bade, V. Saile, G. von Freymann, S. Linden, and M. Wegener, *Science*, 2009, **325**, 1513-1515.
- 114 K. Busch, G. von Freymann, S. Linden, S. F. Mingaleev, L. Tkeshelashvili, and M. Wegener, *Phys. Rep.*, 2007, **444**, 101-202.
- 115 N. Tang, W. Zhong, C. Au, Y. Yang, M. Han, K. Lin, and Y. Du, *J. Phys. Chem. C*, 2008, **112**, 19316-19323.
- 116 A. S. Ivanov, A. J. Morris, K. V. Bozhenko, C. J. Pickard, and A. I. Boldyrev, *Angew. Chem. Int. Ed.*, 2012, **51**, 8330-8333.
- 117 A. K. Jissy and A. Datta, *J. Phys. Chem. Lett.*, 2013, **4**, 1018-1022.

**Biographies and photographs of the authors:**

Meng-Qiang Zhao obtained his PhD in chemical engineering from Tsinghua University (P.R. China) in 2013. He is currently a post-doctoral researcher in the A. J. Drexel Nanomaterials Institute in Drexel University, USA. His research interests are the synthesis and property studies of 3D hierarchical nano-architectures derived from 1D nanowire/nanotubes and 2D flakes, double-helical carbon nanotubes, and carbon nanomaterials for electrochemical energy storage.



Fei Wei obtained his PhD in chemical engineering from China University of Petroleum in 1990. After a postdoctoral fellowship at Tsinghua University, he was appointed an associate professor in 1992 and professor of chemical engineering of Tsinghua University in 1996. He was also a Visiting Professor at Ohio State University, USA, University of Western Ontario, Canada, and Nagoya Institute of Science and Technology, Japan. Now he is the director of the Fluidization Laboratory of Tsinghua University. His scientific interests are chemical reaction engineering, multiphase flow, advanced materials, and sustainable energy. He was awarded Young Particology Research Award for his contributions in the field of powder technology.



Qiang Zhang graduated in 2004 from the department of chemical engineering, Tsinghua University, China, where he continued doing research on mass production of aligned carbon nanotubes and obtained his Ph.D in chemical engineering in 2009. After a short stay as a research associate in Case Western Reserve University, USA in 2009, he joined the Fritz Haber Institute of the Max Planck Society, Germany as a post-doctoral fellow. He was appointed an associate professor of chemical engineering of Tsinghua University in 2011. His current research interests are carbon based hierarchical nanostructures, sustainable chemical engineering, as well as energy conversion and storage (e.g. lithium-sulfur batteries, lithium-ion batteries, and supercapacitors).



Gui-Li Tian obtained her BS degree in 2010 in Chemical Engineering and Technology from Tianjin University and then joined Tsinghua University where she is currently pursuing her PhD in Chemical Engineering. Her research involves the synthesis of nitrogen doped nanocarbons including carbon nanotubes and graphene and their application in energy storage and conversion systems.